Electronic Supplementary Information (ESI) for

Suppressing Barite Crystallization with Organophosphorus Compounds

Ricardo D. Sosa,[1] Jacinta C. Conrad,[1] Michael A. Reynolds,[2] and Jeffrey D. Rimer[1]*

[1] Department of Chemical and Biomolecular Engineering, University of Houston, Houston, Texas 77204, United States
[2] Shell Exploration and Production Company, Houston, TX 77079, USA

*Corresponding author: jrimer@central.uh.edu

Table of Contents

List of Supplementary Figures

Methods

Materials. The following reagents were purchased from Sigma Aldrich: barium chloride dihydrate (99+%), sodium sulfate (>99%), sodium hydroxide (>97%), sodium chloride (>99.5%), diethylene-triaminepentakis(methylphosphonic acid) solution (~50%), and phytic acid dipotassium salt (>99%). All chemicals were used as received without further purification. Silicone tubing was purchased from Cole-Parmer. Deionized (DI) water used in all experiments was filtered with an Aqua Solutions RODI-C-12A purification system (18.2 MΩ·cm).

Bulk crystallization assays. Barite crystals were synthesized using a protocol modified from procedures reported in the literature.[1-6] Barium sulfate crystals were synthesized by first adding $NaCl_{(aq)}$ into a 20-mL glass vial, followed by aliquot addition of 10 mM $BaCl_{2,(aq)}$ and 10 mM $Na_2SO_{4(aq)}$ stock solutions under mild agitation for 10 s. Samples prepared in the presence of molecular modifiers were carried out by adding aliquots of molecular modifiers to the reaction mixture prior to the addition of Na_2SO_4. The final growth solutions had a volume of 10 mL and pH measuring 7.1 ± 0.3 with the following composition: 0.5 mM $BaCl_2$, 0.5 mM Na_2SO_4, 600 mM NaCl, and x nM modifier ($0 \leq x \leq 50$). The crystallization vials were left unperturbed at 21 °C for 24 h to allow crystallization of barite crystals that display (001), (210), and (100) facets.

Microfluidic assays. Inhibition efficacy of modifiers was evaluated by imaging of barite growth over time using an inverted optical microscope. Microfluidic devices were fabricated and seeded with barite crystals using a previously reported method.[7] Two components of growth solutions (S = 7) were prepared and transferred into separate syringes. One solution contained 0.5 mM $BaCl_2$ and the second solution contained 0.5 mM Na_2SO_4, 1.2 M NaCl and various quantities of growth modifiers (0 – 50 nM). The two solutions were mixed using an inline flow configuration that produced a final composition of 0.35 mM $BaCl_2$, 0.35 mM Na_2SO_4, 600 mM NaCl and inhibitors at varied concentration. The fully mixed growth solution was introduced into seeded PDMS chips using a dual syringe pump where inhibitors were added to the syringe containing SO_4^{2-} to minimize formation of modifier-cation complexes. Growth solutions were mixed through silicon tubing attached to a y-connector, and then subsequently fed into the microfluidic chip containing seed crystals.

Materials characterization. To adjust and monitor the solution pH, Dual star benchtop pH/ISE meters (Orion) equipped with a ROSS Ultra electrode (8102BNUWP) were used before and after crystallization. For *ex situ* microscopy measurements, a clean glass slide (0.5×0.5 cm^2) was placed at the bottom of the glass vials to collect barite crystals. The glass slide was removed from its solution after crystallization, then thoroughly rinsed with DI water, and dried in air prior to further analysis. Scanning electron microscope (SEM) samples were prepared by attaching carbon tape to SEM studs and subsequently attaching glass slides to carbon tape by gently pressing the glass slide to the tape using tweezers. Scanning electron microscope (SEM) images were obtained on a FEI 235 dual-beam (focused ion-beam) system operated at an accelerating voltage of 15 kV and a working distance of 5 mm. As-synthesized samples were prepared by gently pressing the glass slide containing crystals onto the carbon tape. All the samples were coated with a thin layer of gold (ca. 5-10 nm) prior to imaging.

Barite crystal size and morphology were examined using a Leica DM2500-M optical microscope in transmittance mode, whereas *in situ* imaging of crystal growth was performed on the Leica DMi8 inverted optical microscope using transmittance mode equipped with HC PL Fluotar 5×, 10×, 20×, and N Plan L 50× objectives. A minimum of ten brightfield images of

representative areas on the bottom of the glass vials were captured in transmittance mode for characterization of crystals grown in the bulk assay. The average [010] length, [100] width, and [001] thickness of crystals in optical micrographs were measured from a minimum of 100 crystals per trial and three separate trials. For *in situ* time-resolved studies, LAS X software was used to program a minimum of 30 positions along a seeded microchannel, at which images were captured in transmittance mode at 5 min intervals for at least 3 h. Crystals observed *in situ* were analyzed using ImageJ (NIH) using a procedure previously reported.[7] At least 90 crystals located in different channels per batch were analyzed at 5 min intervals over a minimum of 3 h. From the change in crystal length over time, a growth rate *r* was determined for each experimental condition, which can be written as percent inhibition using the relative growth rate described previously.

Atomic force microscopy. *In situ* atomic force microscopy (AFM) was performed to examine the temporal changes in topographical features on the (001) surface of barite. An AFM specimen disk (Ted Pella) covered with a thin layer of thermally curable epoxy (Loctite, China) was placed at the bottom of glass vials during barite synthesis in the bulk assay procedure outlined above. The epoxy was first partially cured in an oven for approximately 6 min at 60 °C and then dried in air overnight to fully cure the epoxy. All AFM measurements were performed in a Cypher ES instrument (Asylum Research, Santa Barbara, CA) in contact mode using silicon nitride probes with a spring constant of 0.08 N m^{-1} (Oxford Instruments, PNP-TR 1). The liquid cell (ES-CELL-GAS) contained two ports for inlet and outlet flow to maintain constant supersaturation during AFM measurements. Several concentrations of phytic acid and DTPMP within a nanomolar range were tested in growth solutions with supersaturation ratio S = 5.3. The growth solution was delivered to the liquid cell using an in-line mixing configuration where the two solute solutions (Ba^{2+}, and SO_4^{2-}) were combined immediately before being introduced into the cell (similar to the microfluidics configuration). Freshly prepared growth solutions were used for each experiment (within 2 hours of their preparation). Continuous imaging was performed at ambient temperature in contact mode with a scan rate of 2.44 Hz and 9.77 Hz at 256 lines per scan. Analysis of the (001) barite surface kinetics (relative step velocities) were carried out by measuring the temporal change in 2D island length in the [010] and [100] directions for a minimum of 50 2D islands in the presence of inhibitors (v) and in the absence of inhibitors (v_0).

Nucleation studies. The onset of nucleation and aggregation of particles was characterized by using Nanosight LM10-HS oblique illumination microscopy (OIM) equipped with a green laser (532 nm) illuminating a solution film with a thickness of 500 μm at an oblique angle. This method relies on light scattered at wavevectors of order μm^{-1} and probes length scales in the range 10^{-3} to 10 μm. 1 mL samples of supersaturated solution (S = 10) in the absence and presence of inhibitors are injected into the OIM chamber, creating the 500 μm film between two glass substrates, 30 s after mixing all reagents at room temperature 21 ± 1 °C. The Brownian trajectory, average number density, and size of the particles can be determined through OIM analysis.[8] A minimum of 10 regions within the liquid film were recorded and at least 50 particles were analyzed to obtain particle number density for each inhibitor concentration.

Supplementary Figures

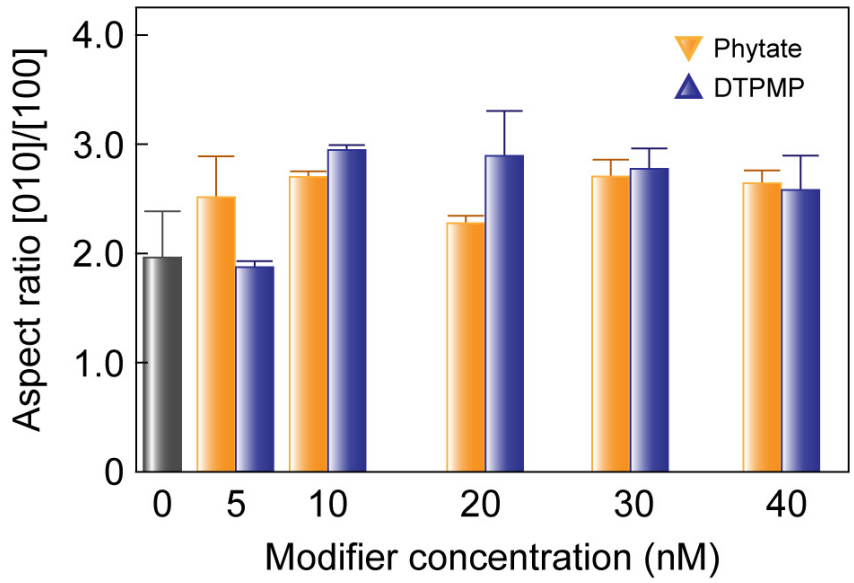

Figure S1. Length to width aspect ratio measurements for barite crystals grown in 24-h bulk assays in supersaturated growth media (S = 10) at room temperature in the presence and absence (gray bar) of inhibitors. Error bar equals one standard deviation.

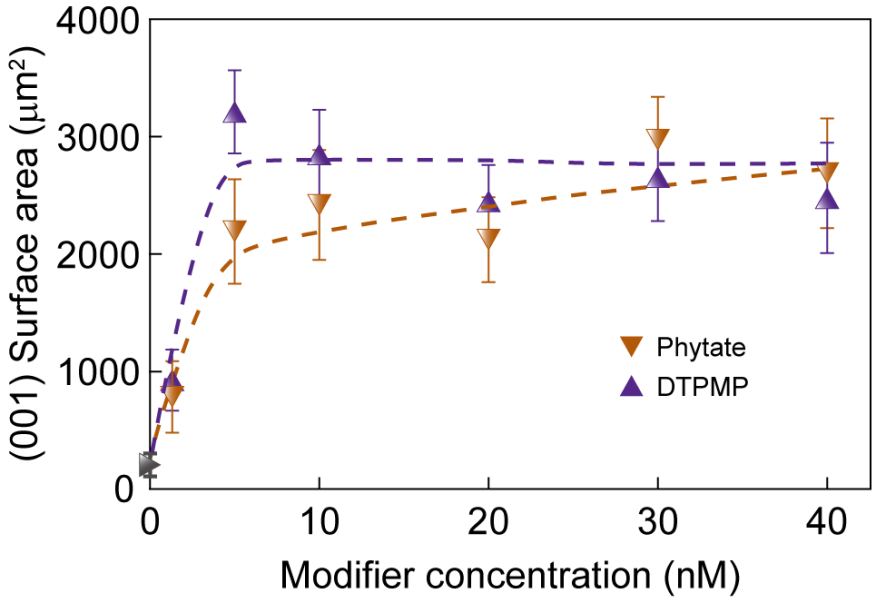

Figure S2. Barite (001) basal surface area measurements of crystals synthesized in quiescent bulk crystallization assays after 24 h using a supersaturated growth solution (S = 10) containing either phytate (orange symbols) or DTPMP (purple symbols) at various concentrations. Dashed lines are interpolated to guide the eye. Error bars span two standard deviations.

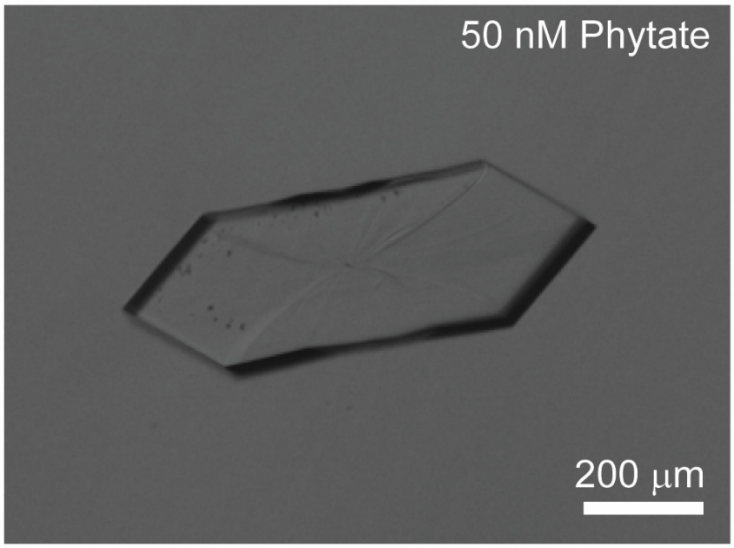

Figure S3. Representative optical micrograph of a barite crystal after a 14 day synthesis at room temperature in supersaturated growth solution (S = 10) containing 50 nM phytate.

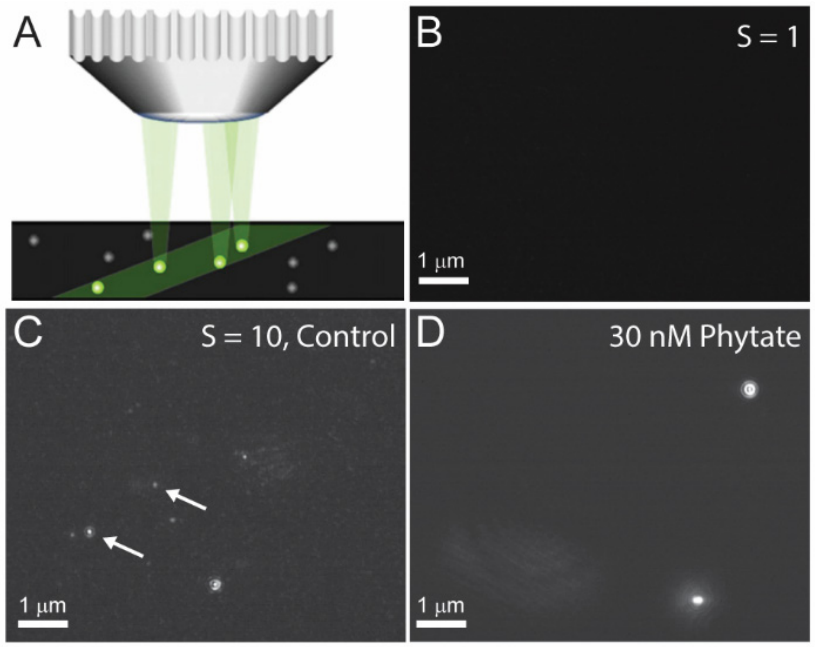

Figure S4. (A) Schematic displaying the oblique illumination microscopy (OIM) setup used for Brownian dynamics measurements to quantify particle number density and size in the absence and presence of inhibitors.[9] (B) Representative image of the thin film chamber filled with a saturated (S = 1) barium sulfate solution after 3 days of mixing reagents. (C) Snapshot of a supersaturated barite solution (S = 10) displaying several particles (image taken 30 min after mixing reagents). (D) Introduction of 30 nM phytate into the growth solution leads to a reduction in particle number density (image taken 30 min after mixing reagents).

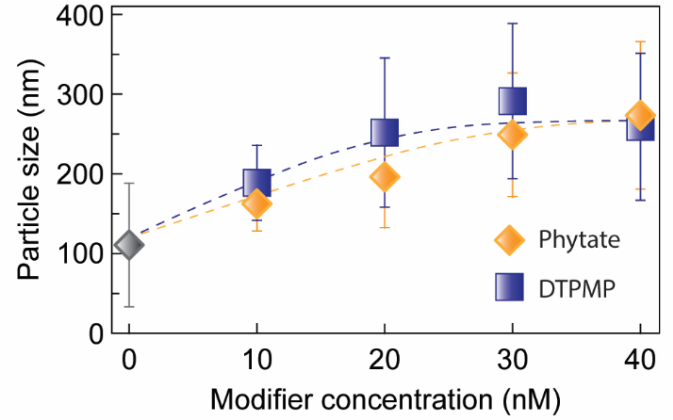

Figure S5. Barium sulfate particle size measured by OIM. Symbols are the average measurements of a minimum of 50 particles (single experiment) for modifier concentrations ≤ 20 nM. Averages at higher modifier content (> 20 nM) are based on at least 10 particles measured for each concentration. Dashed lines are interpolated to guide the eye. Error bars span two standard deviations.

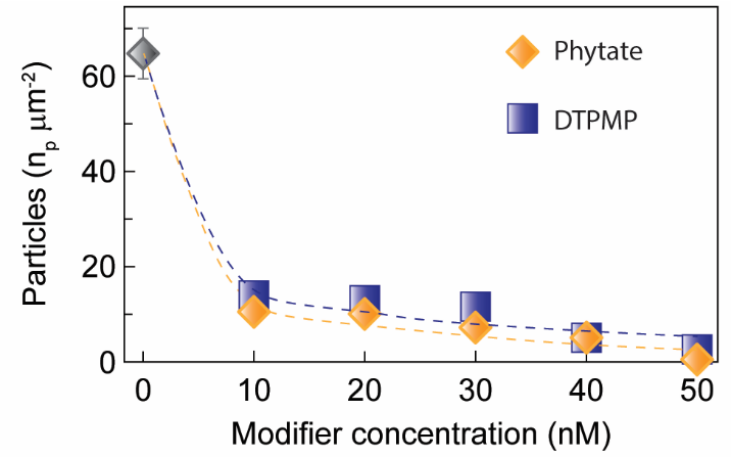

Figure S6. Particle number density of solutions assessed using OIM. Symbols are the average of three individual experiments. Dashed lines are interpolated to guide the eye. Error bar spans two standard deviations and those not shown are smaller than the symbol size.

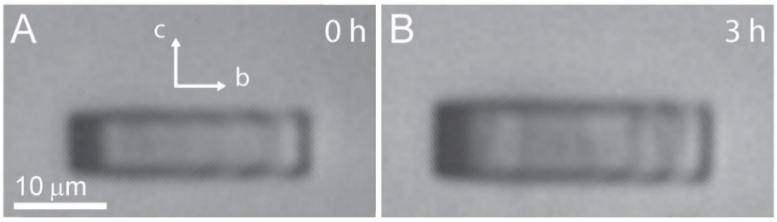

Figure S7. Optical micrographs of barite crystals oriented along the [100] zone axis before (A) and after 3 h (B) exposure to a supersaturated growth solution (S = 7) containing 50 nM PA.

Supplementary Movies

Movie S1. Continuous imaging of a supersaturated (S = 10) barium sulfate solution in the absence of modifier using oblique illumination microscopy (OIM). The Brownian trajectory of barium sulfate particles is observed. The sample was imaged after 30 min of solution preparation, with a total imaging time is 10 s and a frame rate of 25 frames s^{-1}.

Movie S2. Time-resolved brightfield optical microscopy imaging showing the partial inhibition of barite crystal growth in microchannels under flow of a supersaturated (S = 7) solution containing 40 nM phytate. The total imaging time for the video is 3 h with a frame rate of 8 frames s^{-1}.

Movie S3. Time-elapsed sequence of AFM deflection mode images depicting the growth of a barite (001) surface in a supersaturated (S = 5.3) solution where introduction of 400 nM phytate leads to reduced step velocity of advancing layers. Growth solution (with and without modifier) were introduced to the AFM liquid cell at a flow rate of 12 mL h^{-1}. The (001) surface initially becomes populated with triangular-shaped islands bounded by [010] and [120] steps that advance in supersaturated growth solution. The height of each layer corresponds to the dimension of a half unit cell (*c/2*). Upon introducing a growth solution containing phytate, 2D islands become rounded and step advancement is suppressed. The total imaging time for the *in situ* AFM video is 42 min with a frame rate of 6 frames s^{-1}.

References

(1) Nancollas, G. H.; Purdie, N. Crystallization of Barium Sulphate in Aqueous Solution. *Transactions of the Faraday Society* **1963,** *59* (0), 735-740.

(2) Blount, C. W. Synthesis of Barite, Celestite, Anglesite, Witherite, and Strontianite from Aqueous Solutions. *American Mineralogist* **1974,** *59*, 1209-1219.

(3) Liu, S. T.; Nancollas, G. H.; Gasiecki, E. A. Scanning Electron Microscopic and Kinetic Studies of the Crystallization and Dissolution of Barium Sulfate Crystals. *Journal of Crystal Growth* **1976,** *33* (1), 11-20.

(4) Gardner, G. L.; Nancollas, G. H. Crystal Growth in Aqueous Solution at Elevated Temperatures. Barium Sulfate Growth Kinetics. *The Journal of Physical Chemistry* **1983,** *87* (23), 4699-4703.

(5) Black, S. N.; Bromley, L. A.; Cottier, D.; Davey, R. J.; Dobbs, B.; Rout, J. E. Interactions at the Organic/Inorganic Interface: Binding Motifs for Phosphonates at the Surface of Barite Crystals. *Journal of the Chemical Society, Faraday Transactions* **1991,** *87* (20), 3409-3414.

(6) Godinho, J. R. A.; Stack, A. G. Growth Kinetics and Morphology of Barite Crystals Derived from Face-Specific Growth Rates. *Crystal Growth & Design* **2015,** *15* (5), 2064-2071.

(7) Sosa, R. D.; Geng, X.; Reynolds, M. A.; Rimer, J. D.; Conrad, J. C. A Microfluidic Approach for Probing Hydrodynamic Effects in Barite Scale Formation. *Lab on a Chip* **2019,** *19* (9), 1534-1544.

(8) Safari, M. S.; Byington, M. C.; Conrad, J. C.; Vekilov, P. G. Polymorphism of Lysozyme Condensates. *The Journal of Physical Chemistry B* **2017,** *121* (39), 9091-9101.

(9) Safari, M. S.; Wang, Z.; Tailor, K.; Kolomeisky, A. B.; Conrad, J. C.; Vekilov, P. G. Anomalous Dense Liquid Condensates Host the Nucleation of Tumor Suppressor P53 Fibrils. *iScience* **2019,** *12*, 342-355.